AD-A056 099 PENNSYLVANIA STATE UNIV UNIVERSITY PARK APPLIED RESE--ETC F/G 20/11
BEAMLIKE DYNAMIC VIBRATION ABSORBERS,(U)
FEB 77 J C SNOWDON, M A NOBILE
N00017-73-C-1418
UNCLASSIFIED ARL/PSU/TM-77-46
NL

1 OF 1
AD A056 099

END
DATE FILMED
8-78
DDC

# BEAMLIKE DYNAMIC VIBRATION ABSORBERS

by

J. C. Snowdon and M. A. Nobile

Technical Memorandum
File No. TM 77-46
February 17, 1977
Contract No. N00017-73-C-1418

Copy No. 67



The Pennsylvania State University
Institute for Science and Engineering
APPLIED RESEARCH LABORATORY
P. O. Box 30
State College, PA 16801



NAVY DEPARTMENT

NAVAL SEA SYSTEMS COMMAND

This investigation was sponsored by the U.S. Naval Sea Systems Command, Ship Silencing Division, and the U.S. Office of Naval Research.

UNCLASSIFIED

SECURITY CLASSIFICATION OF THIS PAGE (When Data Entered)

| REPORT DOCUMENTATION PAGE | READ INSTRUCTIONS BEFORE COMPLETING FORM |
|---|---|
| 1. REPORT NUMBER: ARL/PSU/TM-77-46 | 2. GOVT ACCESSION NO. / 3. RECIPIENT'S CATALOG NUMBER |
| 4. TITLE (and Subtitle): BEAMLIKE DYNAMIC VIBRATION ABSORBERS, (U) | 5. TYPE OF REPORT & PERIOD COVERED / 6. PERFORMING ORG. REPORT NUMBER |
| 7. AUTHOR(s): J. C. Snowdon and M. A. Nobile | 8. CONTRACT OR GRANT NUMBER(s): N00017-73-C-1418 |
| 9. PERFORMING ORGANIZATION NAME AND ADDRESS: The Pennsylvania State University, Applied Research Laboratory, P. O. Box 30, State College, PA 16801 | 10. PROGRAM ELEMENT, PROJECT, TASK AREA & WORK UNIT NUMBERS: SF43-452-702 (NavSea); N00014-76-RQ-00002 (ONR) |
| 11. CONTROLLING OFFICE NAME AND ADDRESS: Naval Sea Systems Command, Department of the Navy, Washington, DC 20362; Office of Naval Research, Department of the Navy, Arlington, VA 22217 | 12. REPORT DATE: February [illegible], 1977 / 13. NUMBER OF PAGES: 154 |
| 14. MONITORING AGENCY NAME & ADDRESS (if different from Controlling Office): F43452 / SF43452702 | 15. SECURITY CLASS. (of this report): UNCLASSIFIED / 15a. DECLASSIFICATION/DOWNGRADING SCHEDULE |

16. DISTRIBUTION STATEMENT (of this Report)

Approved for public release; distribution unlimited. (as per letter dated March 16, 1977.)

17. DISTRIBUTION STATEMENT (of the abstract entered in Block 20, if different from Report)

18. SUPPLEMENTARY NOTES

19. KEY WORDS (Continue on reverse side if necessary and identify by block number)

Dynamic vibration absorbers.
Bernoulli-Euler beams.
Thin plates.
Viscous damping.
Experimental data.
Solid-type damping.

20. ABSTRACT (Continue on reverse side if necessary and identify by block number)

The performance of several beamlike dynamic vibration absorbers is analyzed and, in one case, confirmed by experiment. The dynamic absorbers are employed to suppress the transmissibility at resonance across a simple mass-spring vibrator, a stanchion, and a simply supported rectangular panel. The absorbers comprise either single or double cantilever beams that are mass loaded at their free ends, or clamped-clamped beams that are centrally mass loaded. Generally, the beams provide both the absorber stiffness and

DD FORM 1 JAN 73 1473 EDITION OF 1 NOV 65 IS OBSOLETE



UNCLASSIFIED

SECURITY CLASSIFICATION OF THIS PAGE (When Data Entered)

391 497

damping--although, once, the beams are considered to possess little damping, and supplemental viscous damping is introduced by dashpots that link the absorber masses to the vibrating primary system of concern. Graphical or tabular design information is specified for the absorbers in each situation considered. Analyses are based throughout on the Bernoulli-Euler beam and thin-plate theories without simplification. In several of the situations analyzed, transmissibility curves are calculated to emphasize that the beamlike absorbers are broadly effective.

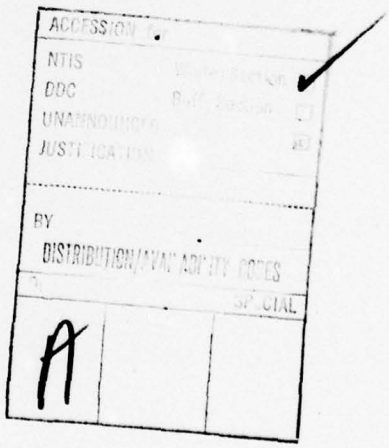

Subject: Beamlike Dynamic Vibration Absorbers

Abstract: Please see page 2

References: Please see pages 23-25

## ABSTRACT

The performance of several beamlike dynamic vibration absorbers is analyzed and, in one case, confirmed by experiment. The dynamic absorbers are employed to suppress the transmissibility at resonance across a simple mass-spring vibrator, a stanchion, and a simply supported rectangular panel. The absorbers comprise either single or double cantilever beams that are mass loaded at their free ends, or clamped-clamped beams that are centrally mass loaded. Generally, the beams provide both the absorber stiffness and damping--although, once, the beams are considered to possess little damping, and supplemental viscous damping is introduced by dashpots that link the absorber masses to the vibrating primary system of concern. Graphical or tabular design information is specified for the absorbers in each situation considered. Analyses are based throughout on the Bernoulli-Euler beam and thin-plate theories without simplification. In several of the situations analyzed, transmissibility curves are calculated to emphasize that the beamlike absorbers are broadly effective.

## INTRODUCTION

The behavior of beamlike dynamic vibration absorbers has been investigated theoretically and, in one case, experimentally. The dynamic absorbers have been tuned initially to suppress the transmissibility at resonance across the one-degree-of-freedom undamped primary system pictured in Fig. 1. Here, a dynamic absorber of mass $M_2$ comprises a mass-loaded double cantilever beam (the beam provides both the absorber stiffness and damping) that is attached to a vibrating item of mass $M_1$. This primary mass is excited by a sinusoidally varying force $\tilde{F}_1$, as in Fig. 1(a), or by a sinusoidally varying ground displacement $\tilde{x}_1$, as in Fig. 1(b).[1] In both cases, $M_1$ resonates on resilient members of total stiffness $K_1$. If the transmissibility T across system (a) is defined as the magnitude of the force ratio $|2\tilde{F}_2/\tilde{F}_1|$, and if the transmissibility across system (b) is defined as the magnitude of the displacement ratio $|\tilde{x}_2/\tilde{x}_1|$--then, at any one frequency,

$$T = |2\tilde{F}_2/\tilde{F}_1| = |\tilde{x}_2/\tilde{x}_1| \quad , \tag{1}$$

where $2\tilde{F}_2$ is the force transmitted to the ideally rigid foundation in Fig. 1(a) and $\tilde{x}_2$ is the displacement of $M_1$ in Fig. 1(b). Thus, the results of a single calculation of transmissibility have dual significance. For a vibrating item of machinery, $M_2/M_1$ would rarely exceed 0.2; whereas, for an instrument mounting, $M_2/M_1$ might be as large as 0.5 or 1.0.

An alternative dynamic absorber is pictured in Fig. 2, where now a centrally mass-loaded clamped-clamped beam is rigidly connected via its

---

[1] Symbols with superior tildes denote quantities that vary sinusoidally with time; symbols with a star superscript represent complex quantities.

terminations to the mass $M_1$ of the undamped primary system. The beams in Figs. 1 and 2 could either be coated with damping compound or could be made from steel/viscoelastic laminations, because such laminates can be produced with the relatively high damping factors needed in many absorber applications. However, for those cases where unusually large damping is required, or where it is not feasible to utilize coated or laminated beams, companion analyses have been made. Thus, the beams of the systems of Figs. 1 and 2 have been assumed to have only slight damping, and viscous damping has been introduced by dashpots that link the concentrated absorber masses to the primary mass $M_1$ in both situations, as indicated in Fig. 3.

The effectiveness of beamlike dynamic absorbers has also been analyzed for primary systems that have distributed mechanical properties. For example, a single mass-loaded cantilever absorber has been applied to reduce the force transmissibility $|\tilde{F}_2/\tilde{F}_1|$ at resonance across an end-driven stanchion of mass $M_S$, as in Fig. 4(a). In addition, a double mass-loaded cantilever absorber has been applied to reduce the force transmissibility at resonance across a simply supported panel of mass $M_p$, as shown in cross section in Fig. 4(b). Here, the force is applied to the panel at any arbitrary location, and the transmitted force $\tilde{F}_2$ comprises four concentrated forces, one at each panel corner, plus a distributed force along the panel boundaries [1][2]. In Fig. 4, as before, the absorber beams are considered to supply both the absorber stiffness and damping.

Graphical or tabular design information has been provided for the foregoing dynamic absorbers in each situation analyzed; thus, curves showing optimum values of the absorber tuning ratios and damping have been plotted

---

[2]Numbers in brackets designate references at end of paper.

versus the mass ratio $M_2/M_1$, $M_2/M_S$, or $M_2/M_P$. Analyses have been made throughout from the Bernoulli-Euler beam theory and from the thin-plate equation without simplification. The results of transmissibility calculations have been presented in several of the situations analyzed to emphasize that the beamlike dynamic absorbers are broadly effective. The practical realization of cantilever beam absorbers is addressed, for example, in [2] - [5]; the design of cantilever beam absorbers that are not mass loaded--so-called "tuned dampers"--is discussed in [6] - [9].

## DOUBLE CANTILEVER ABSORBERS ATTACHED TO A LUMPED MASS-SPRING SYSTEM

### Solid-Type Absorber Damping

The transmissibility across the primary system of Fig. 1 [equation (1)] can be written in general terms as

$$T = \left\{ \{\Omega^2[R(\mu - 1) - \mu] + 1\}^2 + \Omega^4 I^2 (\mu - 1)^2 \right\}^{-\frac{1}{2}} \quad , \tag{2}$$

where

$$\Omega = \omega/\omega_o \tag{3}$$

and

$$\mu = M_1/(M_1 + M_2) \quad . \tag{4}$$

In these equations, R and I are the real and imaginary parts of the normalized driving-point impedance $Z_2/j\omega M_2$ of the dynamic absorber; $\omega$ is angular frequency, hereafter referred to simply as frequency; $\omega_o$ is a reference frequency introduced for convenience such that

$$\omega_o^2 = K_1/(M_1 + M_2) \quad ; \tag{5}$$

and

$$M_2 = (2M + M_b) = (1 + \gamma)M_b \quad , \tag{6}$$

where $M$ is the loading mass at each end of the absorber beam of mass $M_b$ and length 2a. (The masses $M$ have negligible rotary inertia about horizontal axes that are perpendicular to the beam.) It is not difficult to show that

$$(R + jI) = \theta^*/(1 + \gamma)(n^*a) \quad , \tag{7}$$

where

$$\theta^* = \left[\frac{(\text{sh.c.}+\text{ch.s.}) + 2\gamma(n^*a)\text{ch.c.}}{(\text{ch.c.}+1) + \gamma(n^*a)(\text{sh.c.}-\text{ch.s.})}\right]_{(n^*a)} \tag{8}$$

and

$$(n^*a) = (\omega^2\rho a^4/r_g^2E^*)^{1/4} \quad . \tag{9}$$

The abbreviations s.,c., sh., and ch., represent the circular and hyperbolic functions sin $n^*a$, cos $n^*a$, sinh $n^*a$, and cosh $n^*a$, where $n^*$ is the complex beam wavenumber [10]. In addition, $\rho$ is the beam density, $r_g$ is the radius of gyration of the beam cross section, and

$$E^* = E(1 + j\delta_E) \tag{10}$$

is the complex Young's modulus of the beam material, where $j = \sqrt{(-1)}$ and $E$ is the real part, and $\delta_E$ is the ratio of the imaginary to the real part, of the complex modulus. The values of $E$ and $\delta_E$ are assumed to be frequency independent (beam damping of the solid type), so that it is possible to write [10]

$$(n^*a) = na/(1 + j\delta_E)^{1/4} = (p + jq) \quad , \tag{11}$$

where

$$p,q = \pm\, na \left[ \frac{1}{2\sqrt{D_E}} \pm \frac{(1 + D_E^2)^{1/2}}{2\sqrt{2}\, D_E} \right]^{1/2} \tag{12}$$

and

$$D_E = (1 + \delta_E^2)^{1/2} \quad . \tag{13}$$

Finally, the wavenumber $n$ and the frequency ratio $\Omega$ are related as follows:

$$(na)^2 = \frac{N_a^2 \Omega}{(\omega_a/\omega_o)} \quad , \tag{14}$$

where

$$\omega_a = r_g (E/\rho)^{1/2} N_a^2/a^2 \tag{15}$$

is the frequency at which the absorber is tuned to resonate (the first anti-resonant frequency of the beam) and $N_a$ is a number that is dependent on the value of the mass ratio $\gamma = 2M/M_b$. For example, $N_a = 0.87002$, 0.73578, and 0.62051 when $\gamma = 5$, 10, and 20, respectively; other values of $N_a$ can be read off from the solid curve of Fig. 5 for which $0 < \gamma < 20$.

It remains to specify values for the so-called tuning ratio $\omega_a/\omega_o$ and for the damping factor $\delta_E$, which are design parameters of the absorber. Initially, the required values of $\omega_a/\omega_o$ have been taken as those specified as optimum in [10] for absorbers both of the viscous type and of the solid type assumed here; namely,

$$(\omega_a/\omega_o)_{opt} = \sqrt{\mu} \quad . \tag{16}$$

For each value of $\mu$, the required optimum value of $\delta_E$ has been taken as that for which the two peaks in the resultant transmissibility curve [equation (2)] lie on the same horizontal. The appropriate values of $(\omega_a/\omega_o)^2_{opt}$ and $(\delta_E)_{opt}$ are plotted in Fig. 6 for ease of reference. Although $(\delta_E)_{opt}$ has been determined for $\gamma = 10$, little change in $(\delta_E)_{opt}$ or $T_{max}$ results, for example, when $\gamma = 5$ or 20.

Representative transmissibility calculations are plotted on a decibel scale [$20 \log_{10} T(dB)$] in Fig. 7 as the solid curves for which $\mu = 50/51$, 10/11, 5/6, and 2/3 ($M_2/M_1 = 1/50$, 1/10, 1/5, and 1/2, respectively). Because the absorbers are tuned and damped in accordance with the results of Fig. 6, transmissibility is suppressed symmetrically and effectively. For comparison, the dashed curve shows the transmissibility at resonance across the undamped primary system alone ($M_2 = 0$).

The larger values of $M_2/M_1$ in Fig. 6 are accompanied by a requirement for large values of $(\delta_E)_{opt}$, which may not be attainable in all circumstances. Hence, an alternative design approach has also been followed; that is, the more readily attainable values of $\delta_E = 0.1$, 0.2, 0.3, and 0.4 have been assigned to the absorber in turn. Then, for each value of $M_2/M_1$, the tuning ratio $\omega_a/\omega_o$ has been varied ($\neq \sqrt{\mu}$) until the two peaks in the transmissibility curve again lie on the same horizontal. The resultant design data ($\gamma = 10$) appear in Table 1, where it is clear that significantly increased values of $T_{max}$ can result from the use of non-optimum values of $\delta_E$.

## Experimental Results

The effectiveness of various dynamic absorbers with viscous damping has been confirmed in experiments described in [11]. Companion measurements on absorbers with solid-type damping are described here. Although the foregoing

theory relates to an internally damped homogeneous absorber beam, it has provided reasonable agreement with the measured performance of laminated absorber beams damped by viscoelastic materials in configurations that involve either the shear deformation of a central, soft, viscoelastic layer, or the extensional deformation of an outer, stiff, viscoelastic coating. The vibration of such damped beams and plates has been discussed, for example, in [12] - [18].

The damped beams utilized were as follows: a beam comprising a 1.59-mm (1/16-in.) thick layer of Velbex polyvinyl chloride (British Industrial Plastics) sandwiched between two 1.59-mm thick steel strips, and a coated beam comprising a 3.97-mm (5/32-in.) thick layer of LD 400 damping tile (Lord Manufacturing Company) bonded to a single 3.18-mm (1/8-in.) thick steel strip. It was essential that the central layer of the sandwich beam be left free to deform in shear. Consequently, the absorber masses were constructed to permit the two outer steel strips of the beam to move independently of one another. Their design is shown in Fig. 8 and is such that each mass clamps to the top steel strip only, thus permitting the necessary shearing deformation of the central layer. To facilitate absorber tuning, adjustable clamping screws enabled the masses to be repositioned anywhere along the beam. The same masses were used to load the coated beam. The damping factors of the sandwich and coated beams were $\delta_E = 0.29$ and 0.17, respectively; the mass ratios $\mu = M_1/(M_1 + M_2) = 5/6$ and $\gamma = 2M/M_b = 30$ in both cases.

Transmissibility calculations made from Eq. 2 for the foregoing values of $\mu = 5/6$, $\gamma = 30$, $\delta_E = 0.29$ and 0.17, are plotted in Fig. 9 as the solid and dashed curves. Equal transmissibility maxima were obtained in these curves by adjusting the absorber tuning ratio to the values $\omega_a/\omega_o = 0.968$ and 0.988, respectively. The results of transmissibility measurements made

with the absorber beams and the test apparatus described in [11] are plotted in Fig. 10. Good agreement is noted between the measured data and the theoretical curves--which, it should be recalled, relate to homogeneous absorber beams with internal damping. For the sandwich-beam absorber, the values of $T_{max}$ = 11.9 dB and $T_{min}$ = 3.7 dB compare with the predicted values of $T_{max}$ = 12.8 dB and $T_{min}$ = 4.5 dB; for the coated-beam absorber, the values of $T_{max}$ = 15.4 dB and $T_{min}$ = 0.5 dB compare with the predicted values of $T_{max}$ = 16.4 dB and $T_{min}$ = 0 dB. Again, for the sandwich- and coated-beam absorbers, the tuning ratios $\omega_a/\omega_o$ = 0.936 and 0.905 required to achieve equal transmissibility maxima agree reasonably well with theory, differing by approximately 3.3 and 8.4% from their predicted counterparts $\omega_a/\omega_o$ = 0.968 and 0.988.

To conclude, note that the performance of the sandwich-beam absorber was unimpaired when the polyvinyl chloride (PVC) layer in the small central clamped region of the beam (Fig. 1) was replaced by a steel insert [19]--to avoid undue lateral bulging of the PVC and the possible failure of the PVC/metal-interface bonds. Further, note that the performance of the absorber was comparable to that of the conventional dynamic absorber ($\mu$ = 5/6) examined in [11] because, although the transmissibility maxima were 1.4 dB greater here, the intervening transmissibility minimum was more than 5 dB lower than observed previously.

## Viscous Absorber Damping

Consider now the dynamic absorber configuration of Fig. 3(a), where the mass-loaded absorber beam remains as in Fig. 1 but is assumed to have only a small internal damping factor $\delta_E$ = 0.01. Consequently, supplemental damping has been introduced in the form of dashpots that link the concentrated

absorber masses $M$ to the primary mass $M_1$. A damping ratio $\delta_R$ is appropriately defined as

$$\delta_R = \eta/\eta_c \quad , \tag{17}$$

where $\eta$ is the coefficient of viscosity of each dashpot and

$$\eta_c = 2M\omega_a \quad . \tag{18}$$

The general transmissibility equation (2) and the related equations (3) - (15) are directly applicable here, except that the parameter $\theta^*$ of equation (8) has to be redefined as

$$\theta^* = (\text{Num.})/(\text{Den.}) \quad , \tag{19}$$

where

$$(\text{Num.}) = \{2(n^*a)[(3\ \text{ch.c.}-2\ \text{ch.}-2\ \text{c.}+1) + \gamma(n^*a)(\text{sh.c.}-\text{ch.s.})] + \Lambda^*[(\text{sh.c.}+\text{ch.s.}) + 2\gamma(n^*a)\text{ch.c.}]\}_{(n^*a)} \tag{20}$$

and

$$(\text{Den.}) = \{2(n^*a)(\text{sh.c.}-\text{ch.s.}) + \Lambda^*[(\text{ch.c.}+1) + \gamma(n^*a)(\text{sh.c.}-\text{ch.s.})]\}_{(n^*a)} \quad . \tag{21}$$

In these equations

$$\Lambda^* = \frac{j\Omega}{\gamma\delta_R(\omega_a/\omega_o)} \quad , \tag{22}$$

where $(\omega_a/\omega_o)$ and $\delta_R$ are design parameters of the absorber. The values adopted for $\delta_R$ are those established as optimum in [10] for conventional, viscously damped absorbers; namely,

$$(\delta_R)_{opt} \approx [(3/8)(1-\mu)]^{\frac{1}{2}}$$

$$= \frac{1}{2}[(3/8)(1-\mu)]^{\frac{1}{2}} [(1-V)^{\frac{1}{2}} + (1+V)^{\frac{1}{2}}] \quad , \tag{23}$$

where

$$V = \frac{1}{3}\left(\frac{1 - \mu}{1 + \mu}\right)^{\frac{1}{2}} \quad . \tag{24}$$

The companion values of $(\omega_a/\omega_o)_{opt}$ have been taken as those for which the two peaks in the resultant transmissibility curve again lie on the same horizontal. The appropriate values of $(\omega_a/\omega_o)_{opt} \approx \sqrt{\mu}$ and $(\delta_R)_{opt}$ appear in Table 2, which shows that the resultant values of $T_{max}$ fall slightly below those tabulated previously for the absorbers of Fig. 1. Although the new data were obtained for a value of the mass ratio $\gamma = 2M/M_b = 10$, only modest changes in $T_{max}$ were observed, for example, when $\gamma = 5$ and 20.

## 2. CLAMPED-CLAMPED BEAM ABSORBERS ATTACHED TO A LUMPED MASS-SPRING SYSTEM

### Solid-Type Absorber Damping

It is fortunate that the transmissibility across the dynamic absorber system of Fig. 2 is again predicted by equation (2) and that equations (3) - (15) remain relevant with the exception of equations (6) and (8), which become

$$M_2 = (M + M_b) = (1 + \gamma)\, M_b \quad , \tag{25}$$

where M is the single, central mass that now loads the clamped-clamped absorber beam of mass $M_b$ and length 2a, and

$$\theta^* = \left[\frac{2\ \text{sh.s.} + \gamma(n^*a)(\text{sh.c.}+\text{ch.s.})}{(\text{sh.c.}+\text{ch.s.}) + \gamma(n^*a)(\text{ch.c.}-1)}\right]_{(n^*a)} \quad . \tag{26}$$

Although equation (14) is unchanged, new values of $N_a$ = 1.22252, 1.03712, and 0.87607, replace those previously cited when $\gamma$ = 5, 10, and 20; likewise, these values of $N_a$ must be adopted when the mass-loaded absorber beam is designed via equation (15) to resonate at the prescribed frequency $\omega_a$. Other values of $N_a$ are specified by the dashed curve of Fig. 5.

As was true for the double-cantilever absorbers of Fig. 1, values of the tuning ratio $\omega_a/\omega_o$ [equation (14)] have been taken as those given by the simple equation (16), and the required values of the absorber damping factor $(\delta_E)_{opt}$ have been taken as those yielding equal maxima $T_{max}$ in the resultant transmissibility curve. It is an advantage that, when $\gamma = M/M_b = 10$, the values established for $(\delta_E)_{opt}$ and $T_{max}$ are essentially equal to those listed in Table 1 for the absorbers of Fig. 1 under the heading of "Optimum Tuning." Because $(\delta_E)_{opt}$ and $T_{max}$ differ in value from the data of Table 1 by less than - 0.3 and 0.6%, respectively, they have not been tabulated separately.

Viscous Absorber Damping

Attention is now given to the dynamic absorber of Fig. 3(b). Here, the clamped-clamped absorber beam has only slight internal damping ($\delta_E$ = 0.01) and additional damping has been introduced by a dashpot having a

coefficient of viscosity $\eta$ that links the central loading mass $M$ to $M_1$. In this configuration, all equations pertaining to the absorber with no dashpot (Fig. 2) remain relevant with the exception of equation (26) for $\theta^*$, which becomes

$$\theta^* = \left\{ \frac{\zeta^* \Lambda^* - 2(n^*a)[\sigma^* + (\text{sh.c.}+\text{ch.s.}) - 2(\text{sh.}+\text{s.})]}{\sigma^* \Lambda^* - 2(n^*a)(\text{ch.c.}-1)} \right\}_{(n^*a)} , \tag{27}$$

where

$$\zeta^* = [2\ \text{sh.s.} + \gamma(n^*a)(\text{sh.c.}+\text{ch.s.})]_{(n^*a)} , \tag{28}$$

$$\sigma^* = [(\text{sh.c.}+\text{ch.s.}) + \gamma(n^*a)(\text{ch.c.}-1)]_{(n^*a)} , \tag{29}$$

and, as before,

$$\Lambda^* = \frac{j\Omega}{\gamma\delta_R(\omega_a/\omega_o)} , \tag{30}$$

where the damping ratio $\delta_R = (\eta/\eta_c) = \eta/2M\omega_a$.

The values adopted for $\delta_R$ in equation (30) are those drawn from [10] and specified by equation (23) as optimum for the viscously damped absorber of Fig. 3(a). Likewise, the companion values of $(\omega_a/\omega_o)_{opt}$ have been determined as those for which peaks of equal magnitude $T_{max}$ appear in the transmissibility curve. It is again an advantage that the values of $(\omega_a/\omega_o)$ and $T_{max}$ coincide, with less than - 0.2 and + 0.5% discrepancy, with those values set forth in Table 2 for the dynamic absorber of Fig. 3(a).

## SINGLE-CANTILEVER ABSORBER ATTACHED TO A STANCHION

A stanchion of complex wavenumber $n_1^* = (\omega^2\rho_1/r_{g1}^2E_1^*)^{1/4}$, height $\ell_1$, and mass $M_S$, is shown in Fig. 4(a). A horizontal ground force $\tilde{F}_2$ is produced by a horizontal driving force $\tilde{F}_1$ applied to the free end of the stanchion, which is almost undamped. Because $\tilde{F}_2$ becomes untenably large at the fundamental resonance of the stanchion, a cantilever dynamic absorber of complex wavenumber $n_2^* = (\omega^2\rho_2/r_{g2}^2E_2^*)^{1/4}$, length $\ell_2$, and mass

$$M_2 = \gamma_1 M_S$$
$$= (M + M_b) = (1 + \gamma)M_b \qquad (31)$$

has been attached to the driving point. Here, M is the mass that loads the absorber beam of mass $M_b$; and $\rho_i$, $r_{gi}$, and $E_i^* = E_i(1 + j\delta_{Ei})$, are the density, the radius of gyration of the cross section, and the complex Young's modulus, of the stanchion (i = 1) and of the absorber beam (i = 2). As before, it is convenient to write

$$n_i^*\ell_i = (p_i + jq_i) \quad , \qquad (32)$$

where $p_i$ and $q_i$ are defined by equation (12) in which the product na has been replaced by $n_i\ell_i$; in addition, equation (13) becomes

$$D_{Ei} = (1 + \delta_{Ei}^2)^{1/2} \quad , \qquad (33)$$

where $\delta_{E1} = 0.01$, and appropriate values of $\delta_{E2}$ have yet to be determined.

The transmissibility $T = |\tilde{F}_2/\tilde{F}_1|$ across the stanchion, and the relation between the dimensionless products $n_1\ell_1$ and $n_2\ell_2$, can be expressed as follows:

$$T = \left| \frac{(\text{ch.}+\text{c.})}{[(\text{ch.c.}+1) + \Theta^{*}(n_1^{*}\ell_1)(\text{sh.c.}-\text{ch.s.})]} \right|_{(n_1^{*}\ell_1)} \tag{34}$$

and

$$(n_2\ell_2)^2 = \frac{(N_a/N_m)^2}{(\omega_a/\omega_m)} (n_1\ell_1)^2 \quad , \tag{35}$$

where

$$\Theta^{*} = \frac{\gamma_1}{(1+\gamma)(n_2^{*}\ell_2)} \left[ \frac{(\text{sh.c.}+\text{ch.s.}) + 2\gamma(n_2^{*}\ell_2)(\text{ch.c.})}{(\text{ch.c.}+1) + \gamma(n_2^{*}\ell_2)(\text{sh.c.}-\text{ch.s.})} \right]_{(n_2^{*}\ell_2)} \quad . \tag{36}$$

In equation (35), $\omega_m$ is the fundamental resonant frequency of the stanchion for which $N_m = 1.87510$, $\omega_a$ is the frequency to which the dynamic absorber is tuned, and the companion values of $N_a$ are again specified by the solid curve of Fig. 5 (in particular, $N_a = 0.87002$ for the value of $\gamma = M/M_b = 5$ considered here). To obtain the required value of $\omega_a$, the cantilever dynamic absorber can be designed from the equation

$$\omega_a = r_{g2}(E_2/\rho_2)^{\frac{1}{2}} N_a^2/\ell_2^2 \quad . \tag{37}$$

Prior experience with conventional dynamic absorbers attached to distributed mechanical systems [10,20] indicates that optimum values of $(\omega_a/\omega_m)$ and $\delta_{E2}$ can be determined by comparing the transmissibility calculated from equation (34) and the transmissibility

$$T = \left| \frac{(\text{ch.}+\text{c.})}{[(\text{ch.c.}+1) + \gamma_1 (n_1 \ell_1)(\text{sh.c.}-\text{ch.s.})]} \right|_{(n_1 \ell_1)} \tag{38}$$

that is obtained when the absorber is replaced on the stanchion by a lumped mass equal to the absorber mass $M_2$. The transmissibility curves have two points of intersection, which are adjusted by varying $(\omega_a/\omega_m)$ until they lie on the same horizontal when $\delta_{E1} = \delta_{E2} = 0$. The tuning ratio is then said to have attained its optimum value $(\omega_a/\omega_m)_{opt}$. The corresponding value of $(\delta_{E2})_{opt}$ is taken as that for which the transmissibility maxima adjacent to the points of intersection also become equal in level when $\delta_{E1} = 0.01$.

Values of $(\omega_a/\omega_m)^2_{opt}$ and $(\delta_{E2})_{opt}$ that have been determined in the foregoing way are plotted in Fig. 11 for values of the mass ratio $M_2/M_S \leq 0.2$. Values of $(\delta_{E2})_{opt}$ determined for greater mass ratios are not shown because they become unrealistically large. Rather, the damping factor has been assigned the constant values of $\delta_{E2} = 0.4$, 0.6, and 0.8, in turn, and the corresponding quasi-optimum values of the tuning ratio $(\omega_a/\omega_m)$ have been determined as those for which peaks of equal height $T_{max}$ again occur in the transmissibility curve. These values are plotted in Fig. 11 as the solid, dashed, and chain curves, respectively. Although the resultant maximum transmissibility is greater when $M_2/M_S$ is large than it would otherwise be, the increase is not excessive, as the data of Table 3 show.

Representative calculations of transmissibility that have been made from equation (34) are plotted in Fig. 12 as a function of the dimensionless quantity $n_1\ell_1$ which is proportional to $\sqrt{\omega}$. The cantilever absorber is 20% as massive as the stanchion ($\gamma_1 = 0.2$). Two cases have been considered: (1) the absorber has the quasi-optimum tuning ratio $(\omega_a/\omega_m) = 0.764$ and the damping factor $\delta_{E2} = 0.4$ (solid line), and (2) the absorber has optimum

tuning and damping for which $(\omega_a/\omega_m)_o = 0.618$ and $(\delta_{E2})_{opt} = 1.138$ (chain line). The corresponding values of $T_{max}$ are 4.51 and 3.02 (13.1 and 9.6 dB), both of which lie substantially below the value of $T_{max} = 157$ (44 dB) observed when no absorber is attached to the stanchion (dashed curve). It is an advantage that the stanchion resonances at higher frequencies have also been partially suppressed by the absorbers, particularly the third resonance.

## DOUBLE CANTILEVER ABSORBER ATTACHED TO A RECTANGULAR PANEL

Finally considered is the transmissibility T across the rectangular panel of Fig. 4(b) that has sides of lengths u and v, and mass $M_p$. The central double cantilever absorber lies parallel to the longer side u and is identical to the absorber of Fig. 1, having the same length 2a, beam mass $M_b$, mass ratio $\gamma = 2M/M_b$, and total mass $M_2 = (1 + \gamma)M_b$ as before. The impressed force $F_1$ is located at some arbitrary distance $(h_x, h_y)$ from coordinate axes x,y that coincide with one pair of adjacent panel sides u and v. It can be verified that

$$T = \left| \left[ \Psi^* - \frac{\gamma_1 \Xi^* H^*}{\gamma_1 G^* - (R + jI)^{-1}} \right] \right| \quad , \tag{39}$$

where R and I are the real and imaginary parts of the normalized driving-point impedance of the absorber [equation (7)] and

$$\Psi^* = \sum_{k=1,3,5,\ldots}^{\infty} \sum_{m=1,3,5,\ldots}^{\infty} \frac{16(\beta^*)^4}{\pi^2 km\lambda^*} \varphi_{k,m}(h_x, h_y) \quad , \tag{40}$$

$$\Xi^* = \left[ 1 + \sum_{k=1,3,5,\ldots}^{\infty} \sum_{m=1,3,5,\ldots}^{\infty} \frac{16(-1)^{(\theta-1)}}{\pi^2 km\lambda^*} \right] , \tag{41}$$

$$G^* = \sum_{k=1,3,5,\ldots}^{\infty} \sum_{m=1,3,5,\ldots}^{\infty} \frac{4\varphi_{k,m}(h_x,h_y)(-1)^{(\theta-1)}}{\lambda^*} , \tag{42}$$

$$H^* = \sum_{k=1,3,5,\ldots}^{\infty} \sum_{m=1,3,5,\ldots}^{\infty} \frac{4}{\lambda^*} , \tag{43}$$

and

$$\gamma_1 = M_2/M_p . \tag{44}$$

In these equations,

$$\lambda^* = [(\beta^*)^4 - 1] , \tag{45}$$

$$\varphi_{k,m}(h_x,h_y) = \sin k\pi(h_x/u) \sin m\pi(h_y/v) , \tag{46}$$

$$\beta^* = \frac{\pi[k^2 + m^2(u/v)^2]^{\frac{1}{2}}}{n_1^* u} , \tag{47}$$

and

$$\theta = (k + m)/2 , \tag{48}$$

an integer that should not be confused with the complex parameter $\theta^*$ utilized in previous Sections.

The wavenumbers $n_1$ and $n_2$ of the panel and dynamic absorber are related as follows:

$$(n_2 a)^2 = \frac{(N_a/N_m)^2}{(\omega_a/\omega_m)} (n_1 u)^2 \quad , \tag{49}$$

where $\omega_m$ is the fundamental resonant frequency of the panel for which

$$N_m = \pi(u^2 + v^2)^{\frac{1}{2}}/v \quad , \tag{50}$$

and $\omega_a$ is again the absorber frequency for which $N_a = 0.62051$ when $\gamma = 20$, the value assumed here. Other values of $N_a$ are predicted by the solid curve of Fig. 5. Finally, the complex wavenumbers $n_1^*$ and $n_2^*$ are conveniently expressed as

$$n_1^* u = (p_1 + jq_1) \tag{51}$$

and

$$n_2^* a = (p_2 + jq_2) \quad , \tag{52}$$

where $p_1$ and $q_1$, and $p_2$ and $q_2$, are given by equation (12) in which the product na has been replaced by $n_1 u$ and $n_2 a$, respectively. The corresponding damping factors [equation (13)] are $\delta_{E1}$ and $\delta_{E2}$.

Optimum values for the absorber tuning ratio $\omega_a/\omega_m$ and damping factor $\delta_{E2}$ have been chosen by following the approach described in the preceding Section. However, transmissibility calculations made from equation (39) have now been compared with a reference transmissibility

$$T = |\Xi^*/(1 - \gamma_1 H^*)| \tag{53}$$

that pertains when the absorber is replaced on the panel by a lumped mass equal to the absorber mass $M_2 = \gamma_1 M_P$. The driving force $\tilde{F}_1$ is centrally located. The resultant optimum values of absorber tuning and damping for a rectangular panel with $v = u/2$ and $N_m = \sqrt{5}\,\pi$ are plotted in Fig. 13. Because unrealistically large values of $(\delta_{E2})_{opt}$ are called for when $M_2/M_P > 0.15$, they have been omitted; rather, the damping factor has been assigned values established previously as optimum when the absorber was attached to the lumped primary system of Fig. 1. It is these quasi-optimum values of $\delta_{E2}$ that are plotted in Fig. 13 when $M_2/M_P > 0.15$, although the damping factor could again have been assigned constant values, as in Fig. 11. The corresponding values of $(\omega_a/\omega_m)_{opt}$ have once more been taken as those for which peaks of equal height $T_{max}$ (Table 4) appear in the transmissibility curve.

In conclusion, Fig. 14 compares transmissibility calculations (solid and chain curves) made for double cantilever absorbers that are 5 and 50% as massive as the panel, which is assumed to be centrally driven. The absorber tuning ratios and damping factors are $(\omega_a/\omega_m)_{opt} = 0.870$ and $(\delta_{E2})_{opt} = 0.584$, and $\omega_a/\omega_m = 0.554$ and $\delta_{E2} = 0.940$, respectively. The transmissibility without the dynamic absorbers is that shown by the dashed curve. In all cases, the panel damping factor $\delta_{E1} = 0.01$. It is evident that the fundamental panel resonance has been suppressed effectively and symmetrically by the absorbers, and that the panel resonances at higher frequencies have also been suppressed to some extent, particularly by the heavier absorber, which has the larger damping factor.

Although the peak values of transmissibility at the fundamental panel resonance become unequal and different from $T_{max}$ if the panel is driven noncentrally, they remain far smaller than the peak value of $T = 162$ (44 dB) observed when the absorbers are absent. Further, the potential advantage

exists that the excitation of any subsequent panel resonance can be avoided if the noncentral force is located at any point on a nodal line of the particular mode of concern [1].

## ACKNOWLEDGMENTS

The help of Adah A. Wolfe in obtaining the results presented graphically in this paper and of Alan T. Reynard in obtaining the data of reference [19] is acknowledged with gratitude. Samples of LD 400 and polyvinyl chloride were provided by the Lord Manufacturing Company and British Industrial Plastics, Ltd. The investigation was sponsored jointly by the U. S. Naval Sea Systems Command and the U. S. Office of Naval Research.

## REFERENCES


1. Snowdon, J. C., "Forced Vibration of Internally Damped Rectangular and Square Plates with Simply Supported Boundaries," J. Acoust. Soc. Amer., Vol. 56, No. 4, 1974, pp. 1177-1184.

2. Tuplin, W. A., Vibration in Machinery, Sir Isaac Pitman and Sons, Ltd., London, 1940.

3. Allaway, P. H., and Grootenhuis, P., "Unusual Techniques for the Control of Structural Vibration," Paper L36 in Proc. Fifth Intern. Congr. Acoust., 1965, Liege (Fifth ICA Committee, Liege, 1965), Pt. 1(b).

4. Jones, D. I. G., Nashif, A. D., and Adkins, R. L., "Effect of Tuned Dampers on Vibrations of Simple Structures," J. Amer. Inst. Aeronaut. Astronaut., Vol. 5, No. 2, 1967, pp. 310-315.

5. Adams, H. W., Bennett, R. H., Jr., Schendel, J. W., and Van Dyke, J. D., Jr., "Cabin Engine Sound Suppressor," U. S. Patent 3,487,888, January 6, 1970.

6. Jones, D. I. G., Nashif, A. D., and Stargardter, H., "Vibrating Beam Dampers for Reducing Vibrations in Gas Turbine Blades," Journal of Engineering for Power, Trans. ASME, Series A, Vol. 97, No. 1, 1975, pp. 111-116.

7. Jones, D. I. G., Cannon, C. M., and Parin, M. L., "Controlling the Dynamic Response of Jet Engine Components," Shock Vib. Bull., Vol. 45, Pt. 5, 1975, pp. 73-82.

8. Savci, M., "Application of Damper Beams for Lateral Vibrating Systems," Mechanism and Machine Theory Vol. 10, No. 5, 1975, pp. 391-399.

REFERENCES -- CONTINUED

9. Jacquot, R. G., and Foster, J. E., "Optimal Cantilever Dynamic Vibration Absorbers," Journal of Engineering for Industry, Trans. ASME, Series B, Vol. 99, No. , 1977, pp.

10. Snowdon, J. C., Vibration and Shock in Damped Mechanical Systems, John Wiley and Sons, Inc., New York, 1968.

11. Nobile, M. A., and Snowdon, J. C., "Viscously Damped Dynamic Absorbers of Conventional and Novel Design," J. Acoust. Soc. Am., Vol. 61, No. 5, 1977, pp.

12. Ross, D., Ungar, E. E., and Kerwin, E. M., Jr., "Damping of Plate Flexural Vibrations by Means of Viscoelastic Laminae," contribution to Structural Damping, J. E. Ruzicka, ed. (ASME Monograph, American Society of Mechanical Engineers, New York, 1959), Chapter 3, pp. 49-87.

13. Ungar, E. E., "Highly Damped Structures," Machine Design, Vol. 35, No. 4, 1963, pp. 162-168.

14. Agbasiere, J. A., and Grootenhuis, P., "Flexural Vibration of Symmetrical Multilayer Beams with Viscoelastic Damping," J. Mech. Engr. Sci., Vol. 10, No. 3, 1968, pp. 269-281.

15. Grootenhuis, P., "Vibration Control with Viscoelastic Materials," Environmental Engr., Vol. 8, No. 38, 1969, pp. 7-13.

16. Kerlin, R. L., and Snowdon, J. C., "Driving-Point Impedances of Cantilever Beams--Comparison of Measurement and Theory," J. Acoust. Soc. Amer., Vol. 47, No. 1, 1970, pp. 220-228.

17. Lu, Y. P., and Douglas, B. E., "On the Forced Vibrations of Three-Layered Damped Sandwich Beams," J. Sound Vib., Vol. 32, No. 4, 1974, pp. 513-516.

REFERENCES -- CONTINUED

18. Ochs, J. B., and Snowdon, J. C., "Transmissibility Across Simply Supported Thin Plates. I. Rectangular and Square Plates with and without Damping Layers," J. Acoust. Soc. Amer., Vol. 58, No. 4, 1975, pp. 832-840.

19. Reynard, A. T., unpublished data, private communication.

20. Snowdon, J. C., "Vibration of Simply Supported Rectangular and Square Plates to which Lumped Masses and Dynamic Vibration Absorbers Are Attached," J. Acoust. Soc. Amer., Vol. 57, No. 3, 1975, pp. 646-654.

Table 1. Design data for the double cantilever absorber of Fig. 1.

| | Optimum Tuning | | $\delta_E = 0.1$ | | $\delta_E = 0.2$ | | $\delta_E = 0.3$ | | $\delta_E = 0.4$ | |
|---|---|---|---|---|---|---|---|---|---|---|
| $M_2/M_1$ | $(\delta_E)_{opt}$ | $T_{max}$ | $(\omega_a/\omega_o)$ | $T_{max}$ | $(\omega_a/\omega_o)$ | $T_{max}$ | $(\omega_a/\omega_o)$ | $T_{max}$ | $(\omega_a/\omega_o)$ | $T_{max}$ |
| 0.02 | 0.175 | 10.34 | 0.996 | 12.53 | 0.988 | 10.71 | 0.978 | 15.53 | 0.963 | 20.37 |
| 0.03 | 0.215 | 8.48 | 0.996 | 11.74 | 0.987 | 8.49 | 0.976 | 10.42 | 0.962 | 13.66 |
| 0.05 | 0.279 | 6.64 | 0.995 | 11.10 | 0.985 | 7.00 | 0.973 | 6.72 | 0.960 | 8.30 |
| 0.07 | 0.330 | 5.66 | 0.995 | 10.82 | 0.984 | 6.56 | 0.971 | 5.68 | 0.957 | 6.03 |
| 0.10 | 0.397 | 4.80 | 0.995 | 10.61 | 0.984 | 6.16 | 0.969 | 5.02 | 0.953 | 4.80 |
| 0.20 | 0.571 | 3.55 | 0.995 | 10.36 | 0.982 | 5.69 | 0.965 | 4.32 | 0.946 | 3.77 |
| 0.30 | 0.710 | 3.01 | 0.995 | 10.27 | 0.982 | 5.53 | 0.964 | 4.09 | 0.943 | 3.47 |
| 0.50 | 0.945 | 2.51 | 0.995 | 10.20 | 0.982 | 5.40 | 0.962 | 3.91 | 0.940 | 3.24 |

Table 2. Design data for the viscously damped double cantilever absorber of Fig. 3(a).

| $M_2/M_1$ | $(\omega_a/\omega_o)_{opt}$ | $(\delta_R)_{opt}$ | $T_{max}$ |
|---|---|---|---|
| 0.02 | 0.990 | 0.086 | 10.32 |
| 0.03 | 0.986 | 0.104 | 8.44 |
| 0.05 | 0.977 | 0.134 | 6.57 |
| 0.07 | 0.968 | 0.157 | 5.58 |
| 0.10 | 0.955 | 0.185 | 4.70 |
| 0.20 | 0.916 | 0.250 | 3.41 |
| 0.30 | 0.883 | 0.294 | 2.85 |
| 0.50 | 0.826 | 0.353 | 2.31 |

Table 3. Design data for the single cantilever absorber of Fig. 4(a).

| $M_2/M_S$ | $(\delta_{E2})_{opt}$ | $T_{max}$ | $T_{max}$ | | |
|---|---|---|---|---|---|
| | | | $\delta_{E2} = 0.4$ | $\delta_{E2} = 0.6$ | $\delta_{E2} = 0.8$ |
| 0.02 | 0.337 | 7.97 | --- | --- | --- |
| 0.05 | 0.539 | 5.27 | --- | --- | --- |
| 0.10 | 0.778 | 3.93 | 4.89 | 4.10 | 3.93 |
| 0.15 | 0.970 | 3.35 | 4.64 | 3.75 | 3.43 |
| 0.20 | 1.138 | 3.02 | 4.51 | 3.57 | 3.20 |
| 0.30 | --- | --- | 4.36 | 3.38 | 2.97 |
| 0.50 | --- | --- | 4.21 | 3.20 | 2.77 |

Table 4. Design data for the double cantilever absorber of Fig. 4(b).

| $M_2/M_P$ | $T_{max}$ optimum | $M_2/M_P$ | $T_{max}$ quasi-opt. |
|---|---|---|---|
| 0.02 | 8.05 | 0.15 | 4.56 |
| 0.05 | 5.35 | 0.2 | 4.10 |
| 0.10 | 4.11 | 0.3 | 3.58 |
| 0.15 | 3.46 | 0.5 | 3.06 |

## FIGURE LEGENDS

Fig. 1 Vibrating system with springs of total stiffness $K_1$ and mass $M_1$ to which is attached a double cantilever dynamic absorber of mass $M_2$.

Fig. 2 Vibrating mass-spring system with a clamped-clamped beam absorber.

Fig. 3 Vibrating mass-spring system (a) with a viscously damped double cantilever absorber, and (b) with a viscously damped clamped-clamped beam absorber.

Fig. 4 (a) Single cantilever absorber attached to an end-driven stanchion, and (b) section through a double cantilever absorber attached to a rectangular panel driven at an arbitrary point.

Fig. 5 Values of the dimensionless parameter $N_a$ for the double and single cantilever absorbers of Figs. 1 and 4(a) (solid curve), and for the clamped-clamped beam absorbers of Fig. 2 (dashed curve).

Fig. 6 Values of the optimum damping factor and of the square of the optimum tuning ratio for the double cantilever absorber attached to the mass-spring system of Fig. 1. Mass ratio $\gamma = 2M/M_b = 10$.

Fig. 7 Transmissibility across the mass-spring system of Fig. 1 with double cantilever absorbers tuned and damped as specified in Fig. 6. Absorber mass ratios $\mu$ = 50/51, 10/11, 5/6, and 2/3 ($M_2/M_1$ = 1/50, 1/10, 1/5, and 1/2).

Fig. 8 Laminated absorber beam with a loading mass that clamps to only one of the outer steel strips, thus leaving the central visco-elastic (PVC) layer free to shear.

FIGURE LEGENDS -- CONTINUED

Fig. 9 Transmissibility across the mass-spring system of Fig. 1 when the mass ratios $\mu = 5/6$ and $\gamma = 30$. For the solid and dashed curves, the absorber damping factors $\delta_E = 0.29$ and 0.17, respectively.

Fig. 10 Measured transmissibility across the mass-spring system of Fig. 1(b) when $\mu = 5/6$ and $\gamma = 30$. Solid curve refers to a PVC sandwich beam (Fig. 8) for which $\delta_E = 0.29$; the dashed curve refers to a LD 400 coated beam for which $\delta_E = 0.17$.

Fig. 11 Values of the optimum damping factor and of the square of the optimum tuning ratio for the single cantilever absorber attached to the stanchion of Fig. 4(a). Mass ratio $\gamma = M/M_b = 5$.

Fig. 12 Transmissibility across the stanchion of Fig. 4(a) with the single cantilever absorber tuned and damped as specified in Fig. 11. Absorber mass ratio $\gamma_1 = M_2/M_S = 0.2$. For all curves, the stanchion damping factor $\delta_{E1} = 0.01$; for the dashed curve, $\gamma_1 = 0$.

Fig. 13 Values of the optimum damping factor and of the square of the optimum tuning ratio for the double cantilever absorber attached to the panel of Fig. 4(b) when the panel is driven centrally. Mass ratio $\gamma = 2M/M_b = 20$.

Fig. 14 Transmissibility across the panel of Fig. 4(b) with the double cantilever absorber tuned and damped as specified in Fig. 13. Absorber mass ratio $\gamma_1 = 0.05$ and 0.5. For all curves, the panel damping factor $\delta_{E1} = 0.01$; for the dashed curve, $\gamma_1 = 0$.

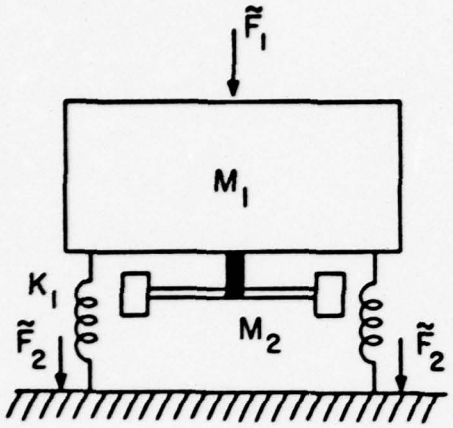


(a)

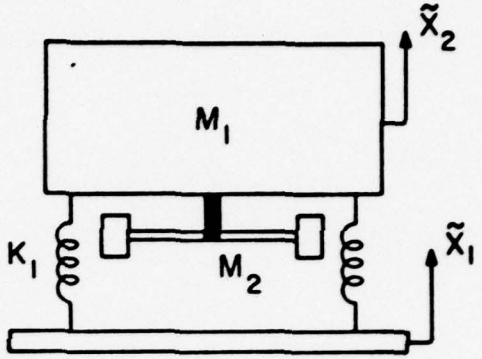


(b)

FIG.1

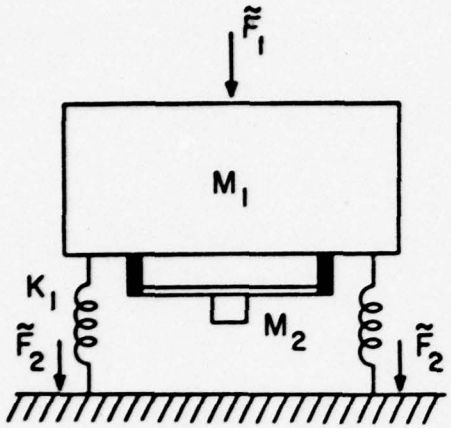


(a)

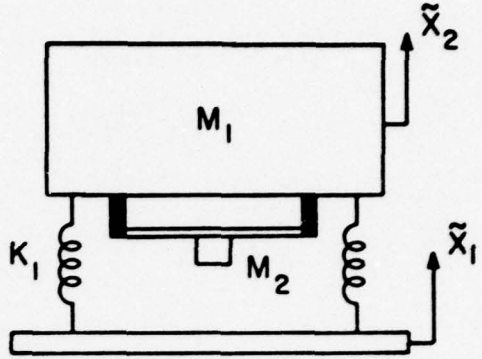


(b)

FIG. 2

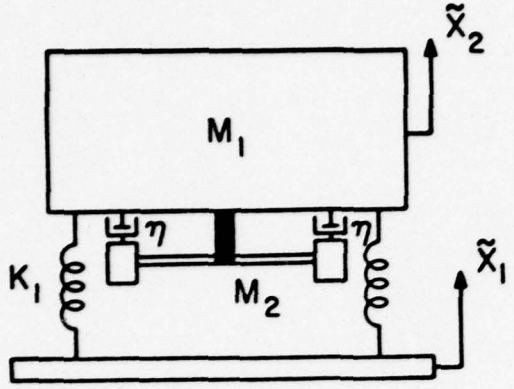
$\tilde{X}_2$
$M_1$
$\eta$
$\eta$
$K_1$
$M_2$
$\tilde{X}_1$

(a)

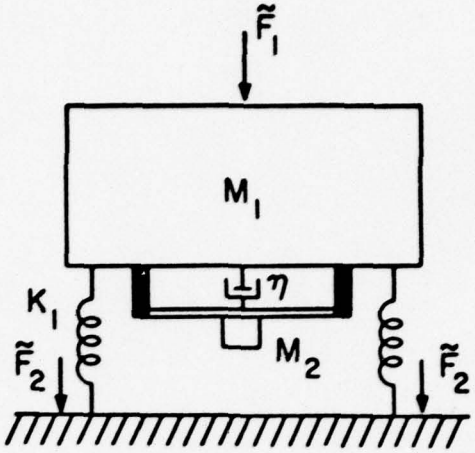
$\tilde{F}_1$
$M_1$
$K_1$
$\eta$
$M_2$
$\tilde{F}_2$
$\tilde{F}_2$

(b)

FIG. 3

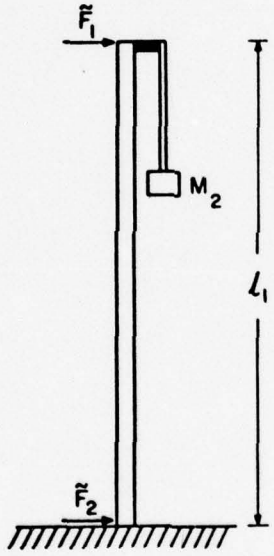


FIG.4(a)

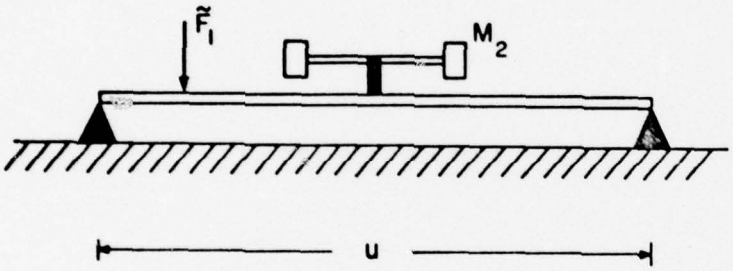


FIG.4(b)

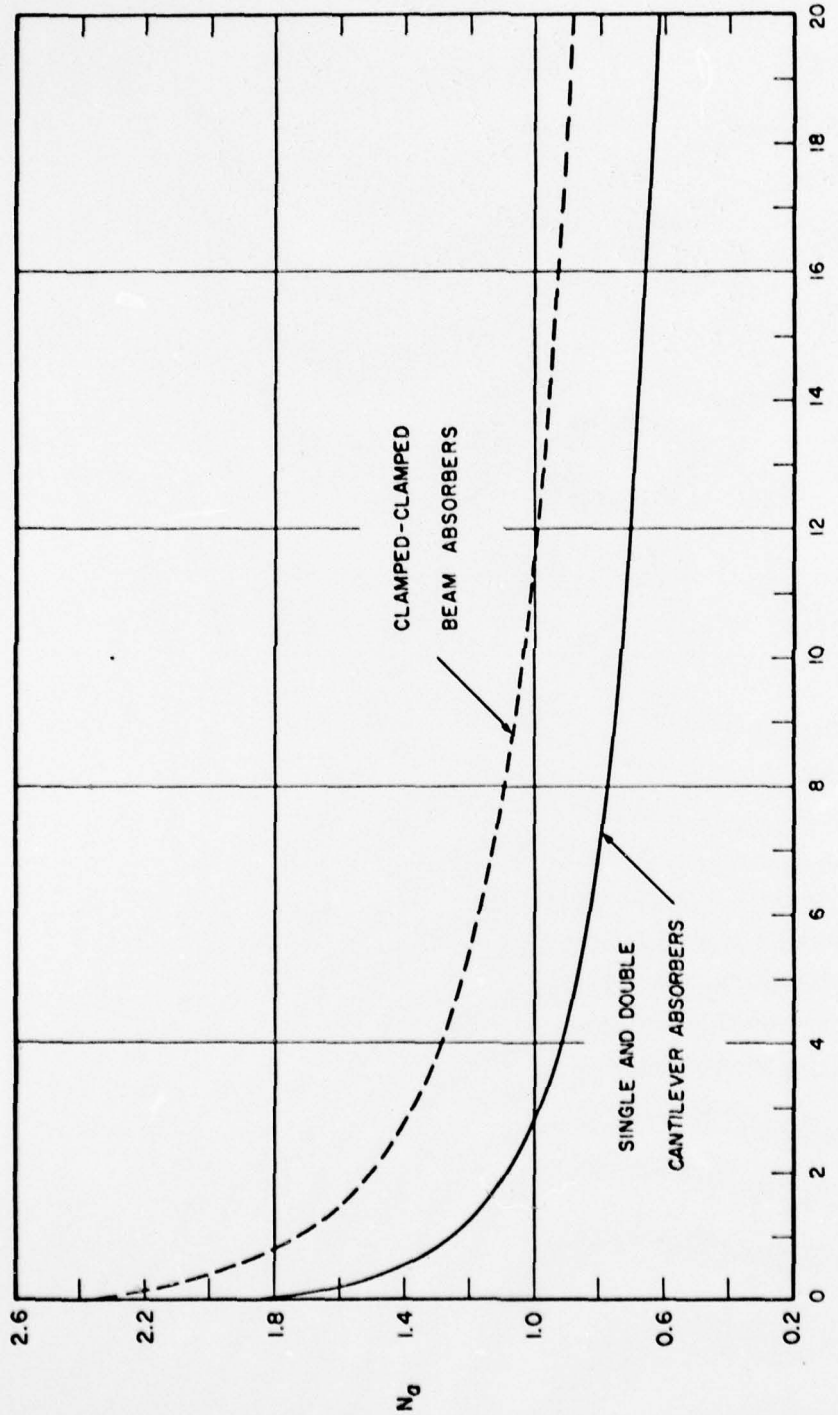
2.6
2.2
1.8
1.4
1.0
0.6
0.2
$N_0$
0
2
4
6
8
10
12
14
16
18
20
MASS RATIO $\gamma$
CLAMPED-CLAMPED
BEAM ABSORBERS
SINGLE AND DOUBLE
CANTILEVER ABSORBERS

FIG. 3

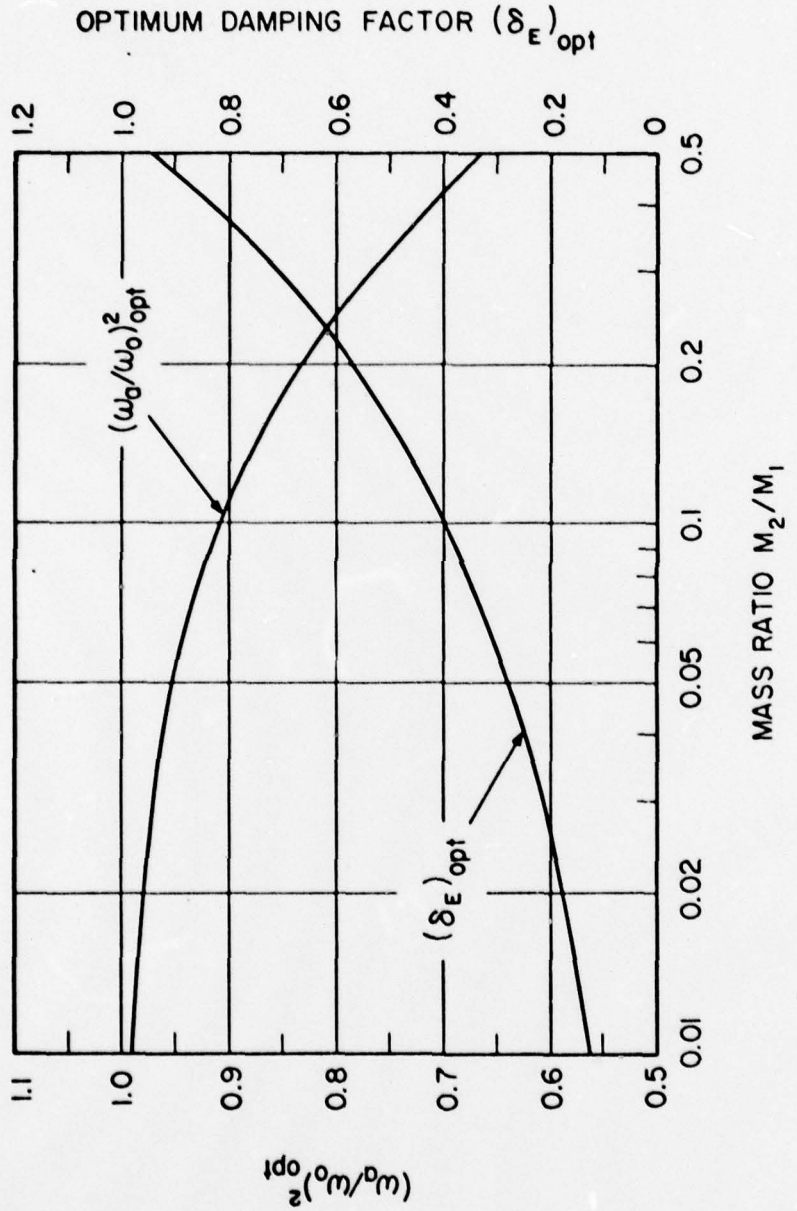
OPTIMUM DAMPING FACTOR $(\delta_E)_{opt}$
1.2
1.0
0.8
0.6
0.4
0.2
0
0.5
0.2
0.1
0.05
0.02
0.01
MASS RATIO $M_2/M_1$
$(\omega_b/\omega_0)^2_{opt}$
$(\delta_E)_{opt}$
1.1
1.0
0.9
0.8
0.7
0.6
0.5
$(\omega_a/\omega_0)^2_{opt}$

FIG. 6

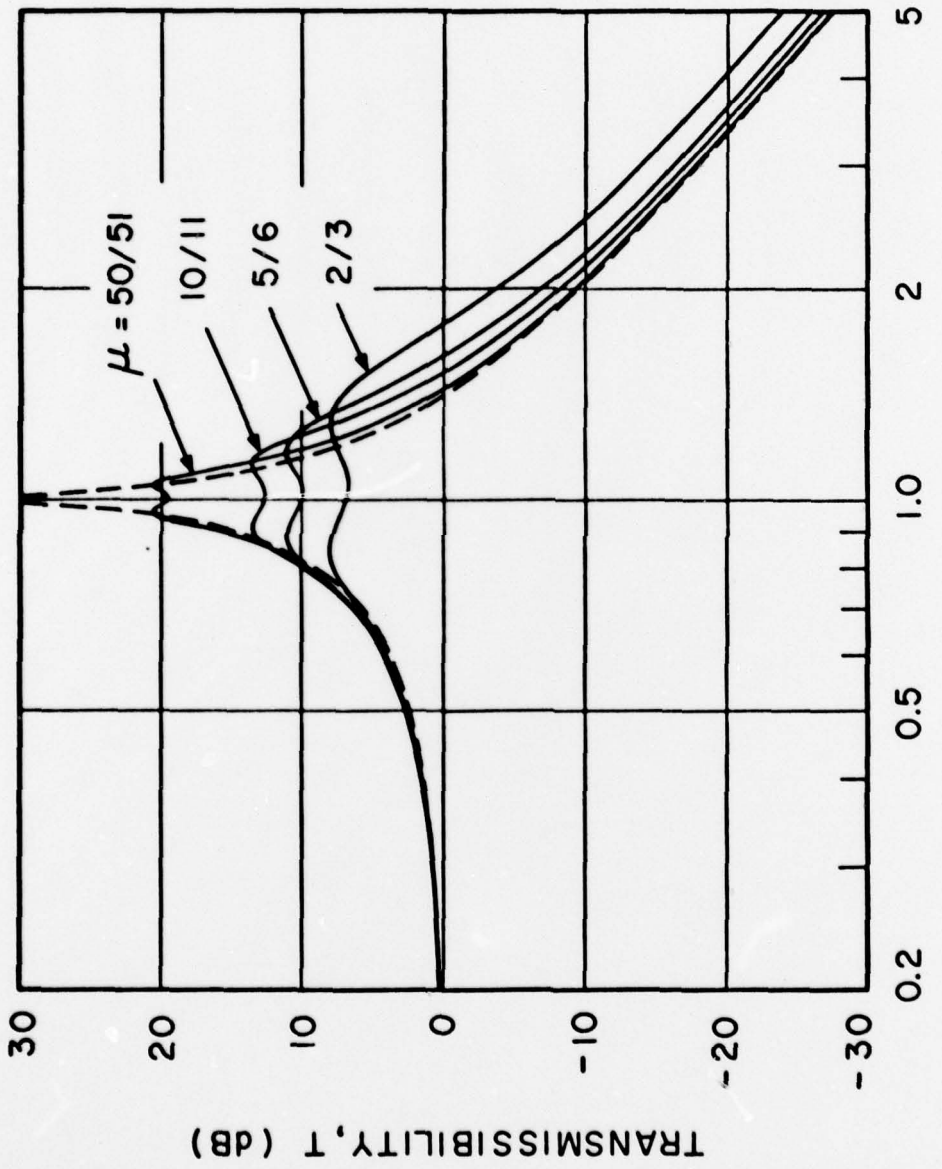
TRANSMISSIBILITY, T (dB)
30
20
10
0
-10
-20
-30
0.2
0.5
1.0
2
5
FREQUENCY RATIO Ω
μ = 50/51
10/11
5/6
2/3

FIG.7

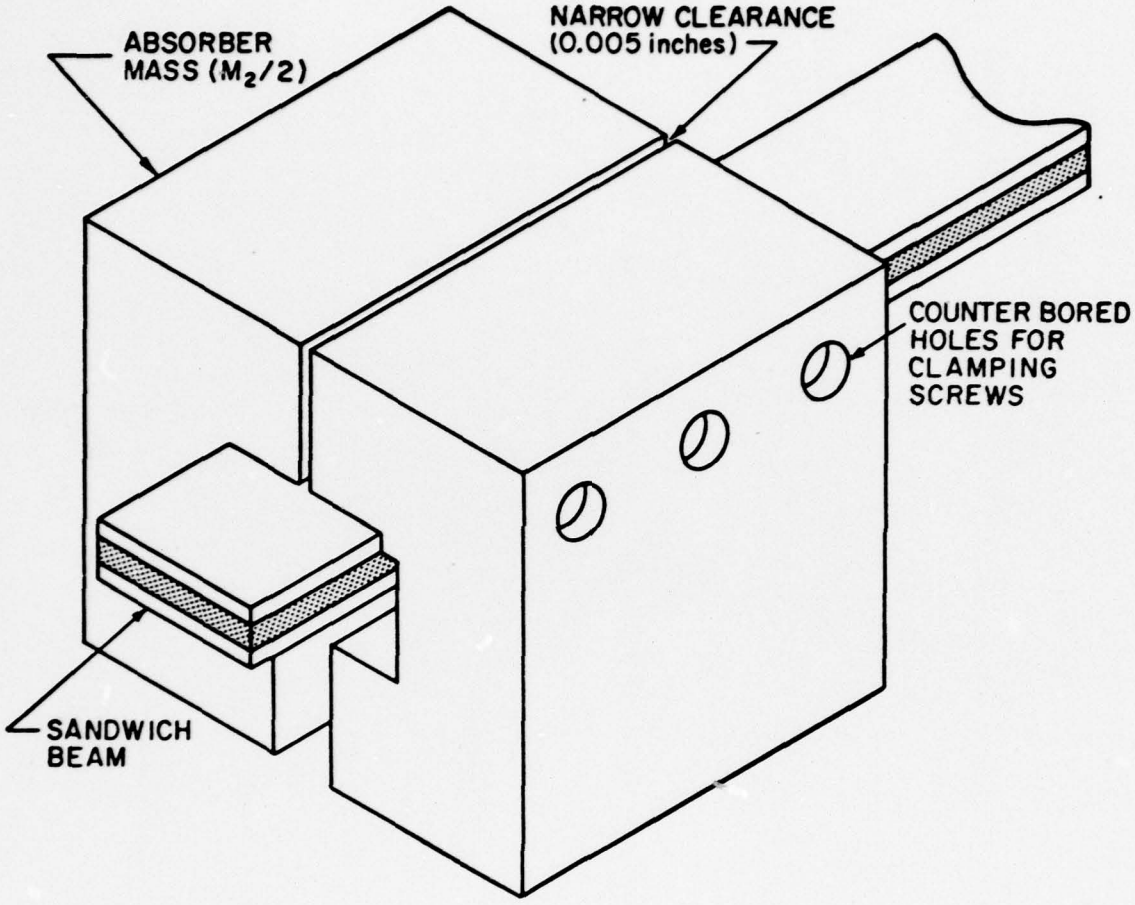
ABSORBER
MASS ($M_2/2$)
NARROW CLEARANCE
(0.005 inches)
COUNTER BORED
HOLES FOR
CLAMPING
SCREWS
SANDWICH
BEAM

FIG.8

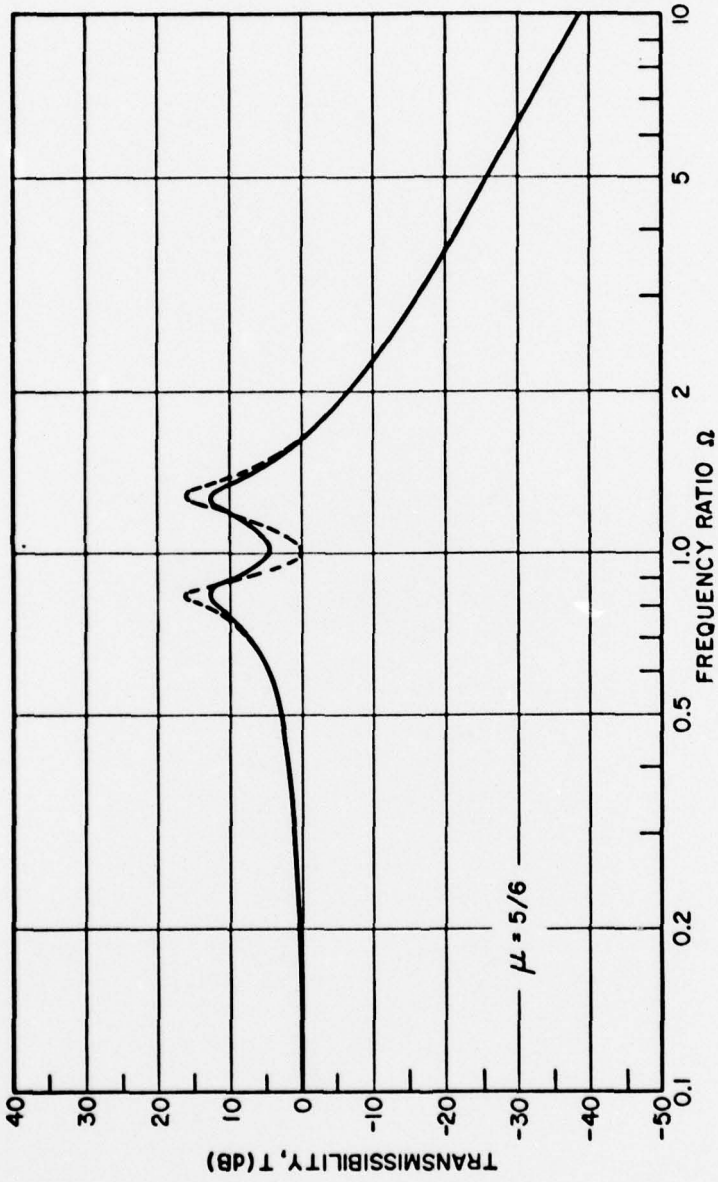
TRANSMISSIBILITY, T (dB)
40
30
20
10
0
-10
-20
-30
-40
-50
0.1
0.2
0.5
1.0
2
5
10
FREQUENCY RATIO Ω
μ = 5/6

FIG. 9

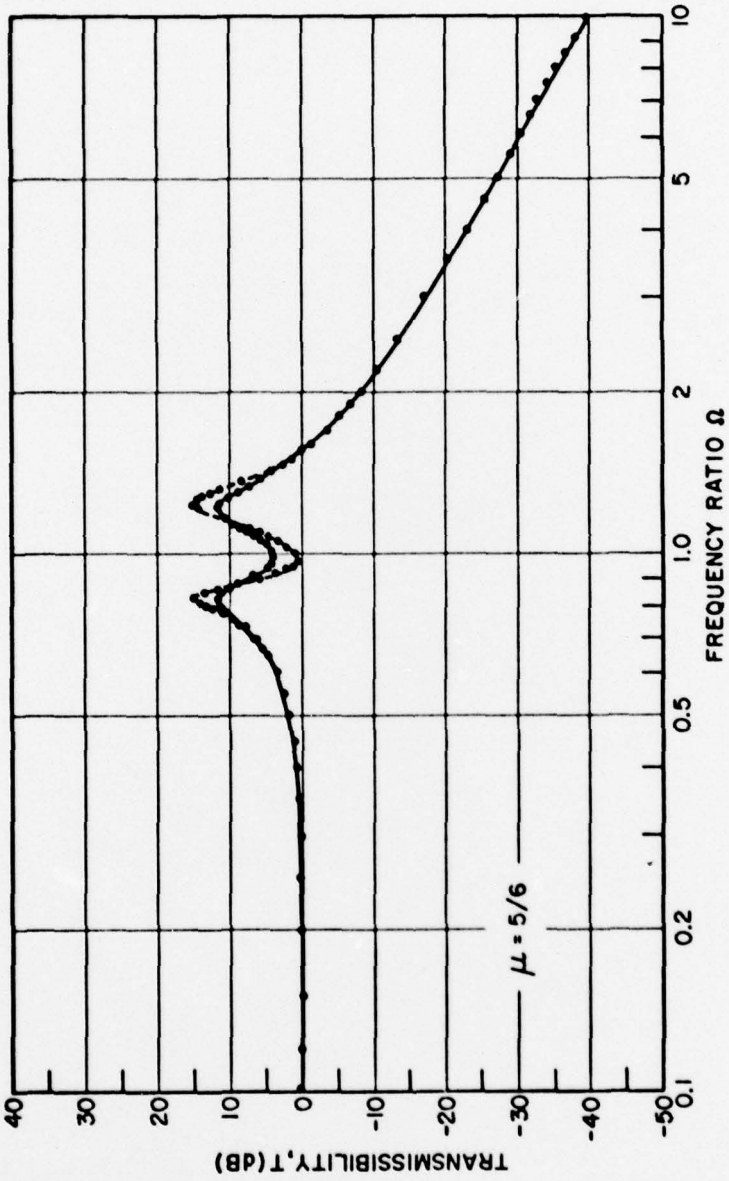
TRANSMISSIBILITY, T (dB)
40
30
20
10
0
-10
-20
-30
-40
-50
0.1
0.2
0.5
1.0
2
5
10
FREQUENCY RATIO Ω
μ = 5/6

FIG.10

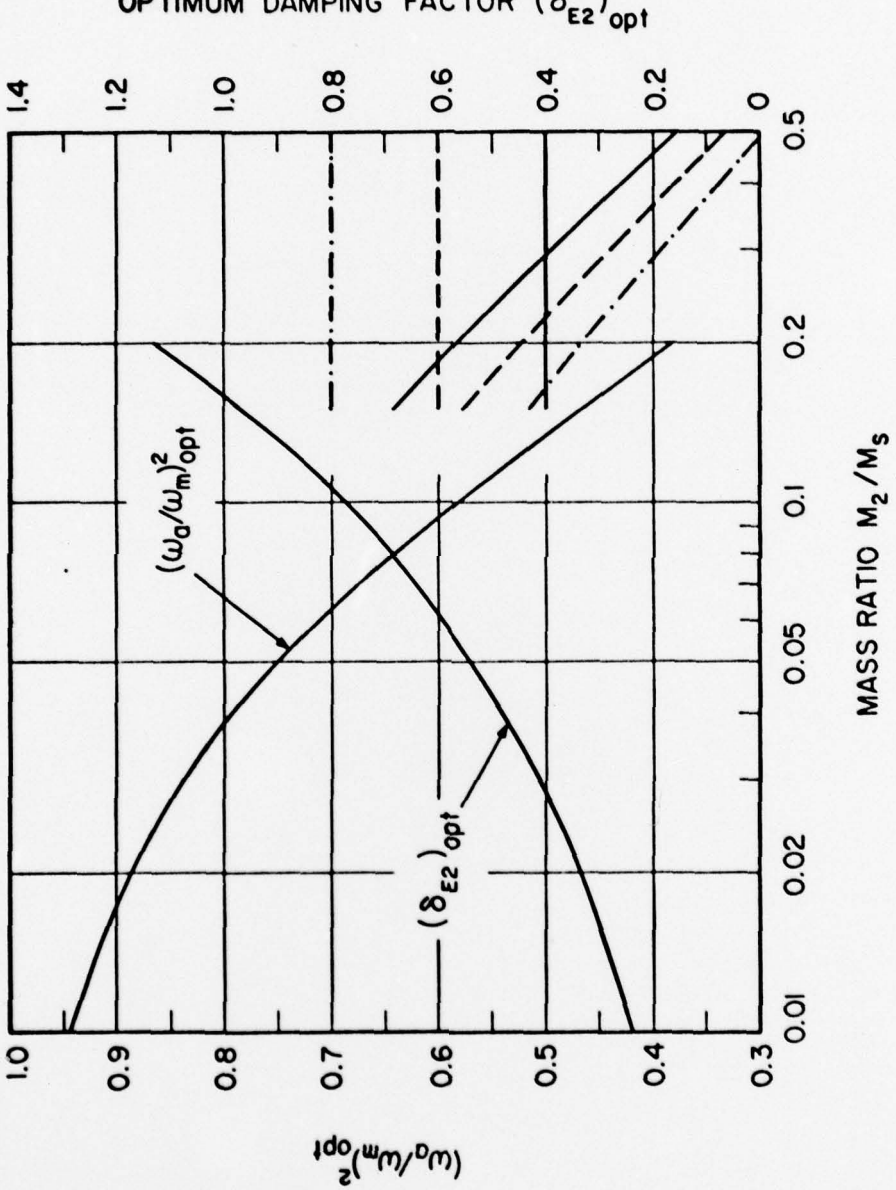
OPTIMUM DAMPING FACTOR $(\delta_{E2})_{opt}$
1.4
1.2
1.0
0.8
0.6
0.4
0.2
0
0.5
0.2
0.1
0.05
0.02
0.01
MASS RATIO $M_2/M_s$
$(\omega_a/\omega_m)^2_{opt}$
$(\delta_{E2})_{opt}$
1.0
0.9
0.8
0.7
0.6
0.5
0.4
0.3
$(\omega_a/\omega_m)^2_{opt}$

FIG.11

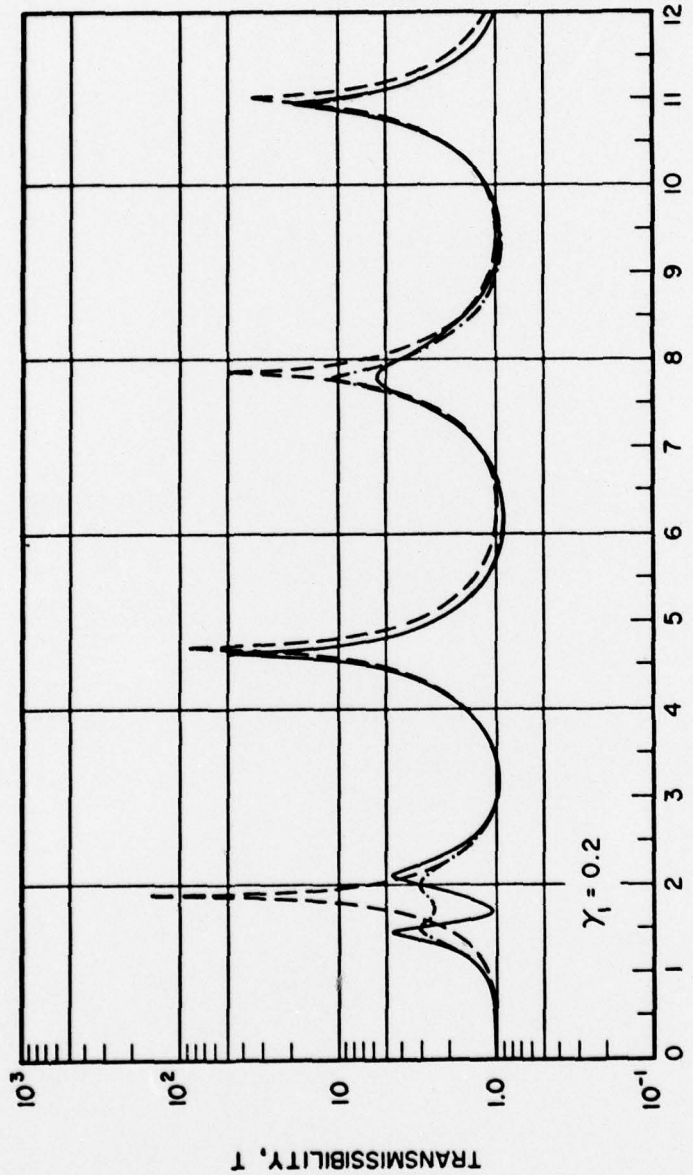
TRANSMISSIBILITY, T
$10^3$
$10^2$
10
1.0
$10^{-1}$
0
1
2
3
4
5
6
7
8
9
10
11
12
$\gamma_1 = 0.2$
$n_1 L_1 \alpha \sqrt{\omega}$

FIG.12

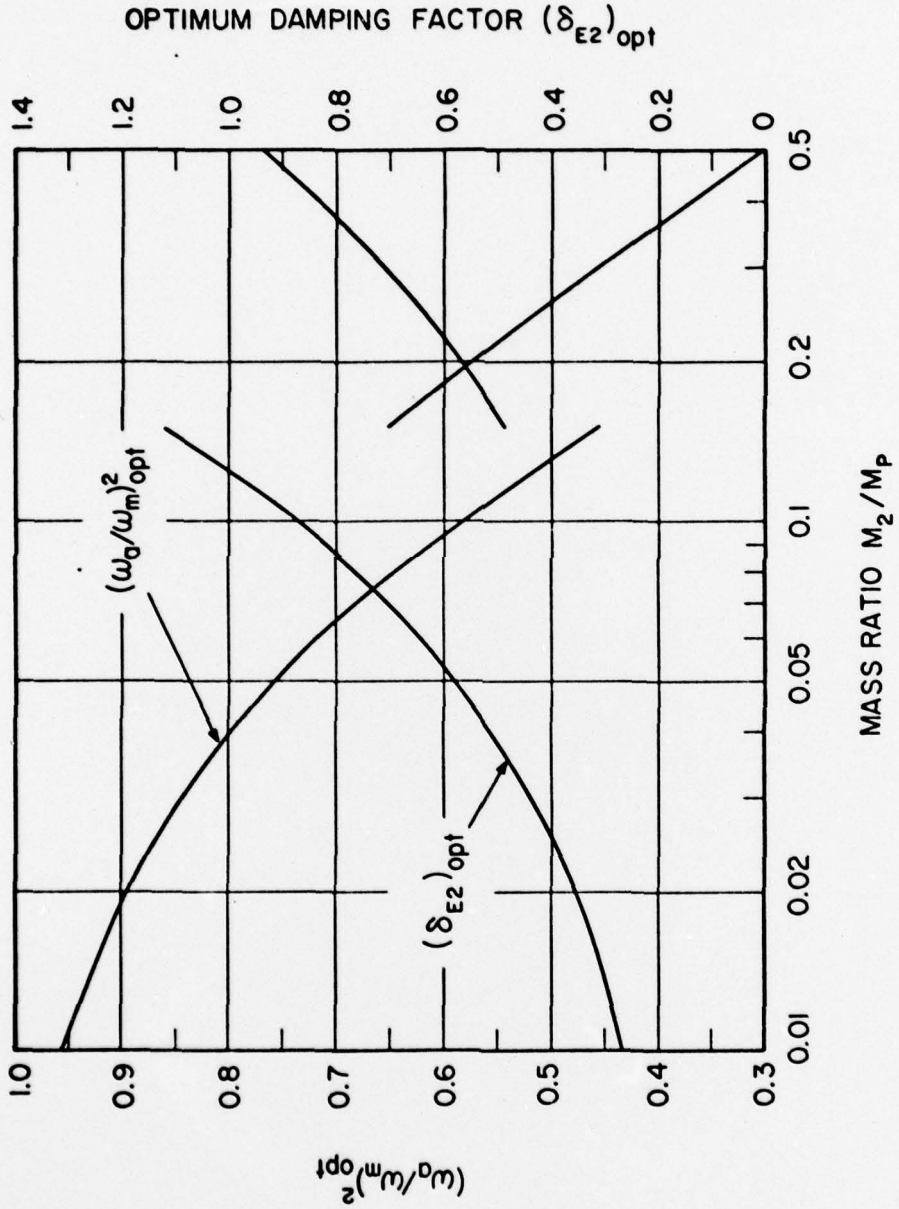
OPTIMUM DAMPING FACTOR $(\delta_{E2})_{opt}$
1.4
1.2
1.0
0.8
0.6
0.4
0.2
0
0.5
0.2
0.1
0.05
0.02
0.01
MASS RATIO $M_2/M_P$
$(\omega_a/\omega_m)^2_{opt}$
$(\omega_a/\omega_m)^2_{opt}$
$(\delta_{E2})_{opt}$
1.0
0.9
0.8
0.7
0.6
0.5
0.4
0.3

FIG.13

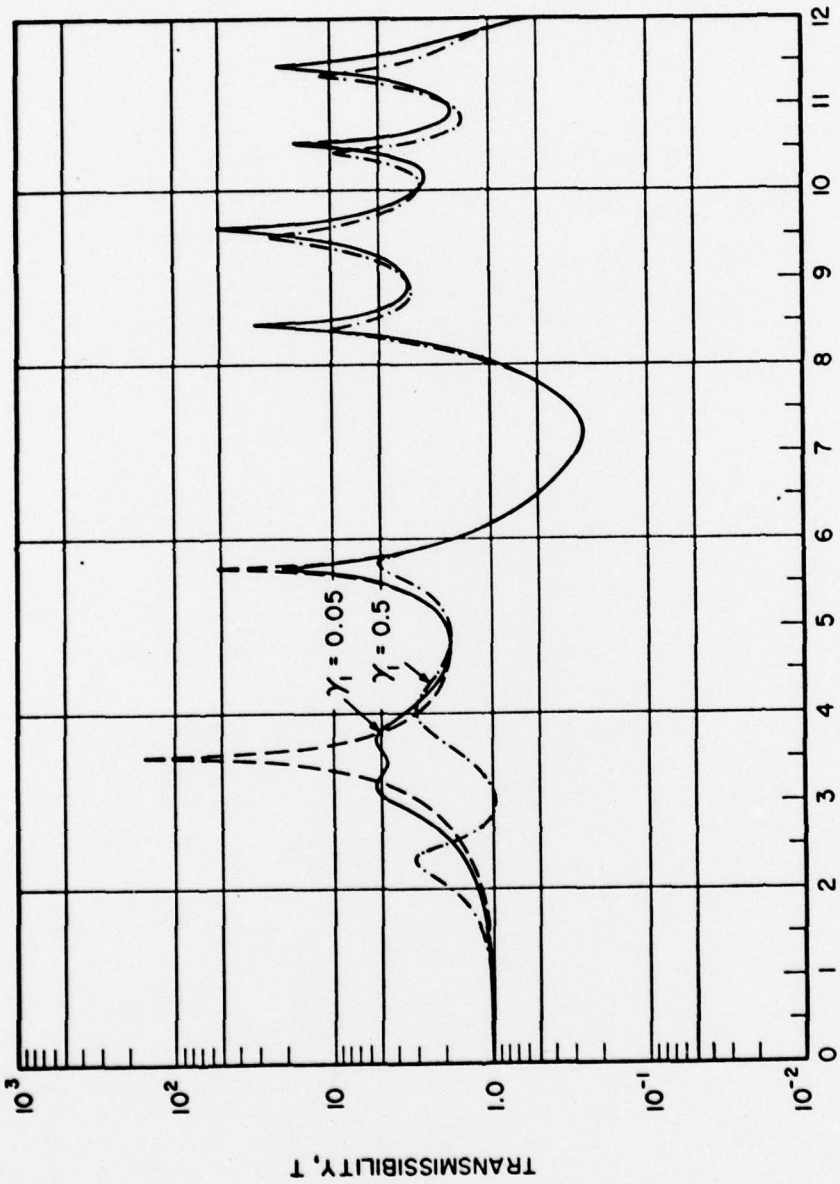
TRANSMISSIBILITY, T
$10^3$
$10^2$
10
1.0
$10^{-1}$
$10^{-2}$
0
1
2
3
4
5
6
7
8
9
10
11
12
$(n_1 u/2) \propto \sqrt{\omega}$
$\gamma_1 = 0.05$
$\gamma_1 = 0.5$

FIG.14

DISTRIBUTION LIST FOR UNCLASSIFIED TM 77-46

Commander
Naval Sea Systems Command
Department of the Navy
Washington, DC 20362
Attn: SEA 924N
(Copy No. 1)

Commander
Naval Sea Systems Command
Department of the Navy
Washington, DC 20362
Attn: PMS-393
(Copy No. 2)

Commander
Naval Sea Systems Command
Department of the Navy
Washington, DC 20362
Attn: PMS-395
(Copy No. 3)

Commander
Naval Sea Systems Command
Department of the Navy
Washington, DC 20362
Attn: PMS-396
(Copy No. 4)

Commander
Naval Sea Systems Command
Department of the Navy
Washington, DC 20362
Attn: Mr. Stephen M. Blazek
SEA 0371
(Copy Nos. 5, 6, 7, 8)

Commander
Naval Sea Systems Command
Department of the Navy
Washington, DC 20362
Attn: Mr. Stephen G. Wieczorek
SEA 037T
(Copy Nos. 9 and 10)

Commander
Naval Sea Systems Command
Department of the Navy
Washington, DC 20362
Attn: Mr. C. C. Taylor
SEA 0372
(Copy Nos. 11 and 12)

Commander
Naval Ship Engineering Center
Center Building
Prince George's Center
Hyattsville, MD 20782
Attn: NAVSEC 6103E
(Copy Nos. 13 and 14)

Commander
Naval Ship Engineering Center
Center Building
Prince George's Center
Hyattsville, MD 20782
Attn: NAVSEC 6105C
(Copy Nos. 15 and 16)

Commander
Naval Ship Engineering Center
Center Building
Prince George's Center
Hyattsville, MD 20782
Attn: Mr. Kenneth G. Hartman
NAVSEC 6105N
(Copy Nos. 17, 18, 19, 20, 21, 22)

Commander
Naval Ship Engineering Center
Center Building
Prince George's Center
Hyattsville, MD 20782
Attn: NAVSEC 6111B
(Copy Nos. 23 and 24)

Commander
Naval Ship Engineering Center
Center Building
Prince George's Center
Hyattsville, MD 20782
Attn: NAVSEC 6111D
(Copy Nos. 25 and 26)

Commander
Naval Ship Engineering Center
Center Building
Prince George's Center
Hyattsville, MD 20782
Attn: NAVSEC 6113C
(Copy Nos. 27 and 28)

Commander
Naval Ship Engineering Center
Center Building
Prince George's Center
Hyattsville, MD 20782
Attn: NAVSEC 6113D
(Copy Nos. 29 and 30)

Commander
Naval Ship Engineering Center
Center Building
Prince George's Center
Hyattsville, MD 20782
Attn: NAVSEC 6120
(Copy Nos. 31 and 32)

Commander
Naval Ship Engineering Center
Center Building
Prince George's Center
Hyattsville, MD 20782
Attn: NAVSEC 6129
(Copy Nos. 33 and 34)

Naval Ship Research and Development Center
Annapolis Division
Annapolis, MD 21402
Attn: Mr. J. Smith
(Copy No. 35)

Naval Ship Research and Development Center
Annapolis Division
Annapolis, MD 21402
Attn: Mr. L. J. Argiro
(Copy Nos. 36, 37, 38, 39, 40, 41)

Naval Ship Research and Development Center
Bethesda, MD 20084
Attn: Dr. M. Sevik
Code 19
(Copy Nos. 42 and 43)

Naval Ship Research and Development Center
Bethesda, MD 20084
Attn: Dr. W. W. Murray
Code 17
(Copy Nos. 44 and 45)

Naval Ship Research and Development Center
Bethesda, MD 20084
Attn: Dr. M. Strasberg
Code 1901
(Copy No. 46)

Naval Ship Research and Development Center
Bethesda, MD 20084
Attn: Dr. G. Maidanik
Code 1902
(Copy No. 47)

Naval Ship Research and Development Center
Bethesda, MD 20084
Attn: Dr. G. Chertock
Code 1903
(Copy No. 48)

Naval Ship Research and Development Center
Bethesda, MD 20084
Attn: Dr. D. Feit
Code 196
(Copy Nos. 49, 50, 51, 52, 53, 54)

Naval Ship Research and Development Center
Bethesda, MD 20084
Attn: Dr. J. T. Shen
Code 1942
(Copy No. 55)

Director
Defense Documentation Center
Cameron Station
Alexandria, VA 22314
(Copy Nos. 56, 57, 58, 59, 60, 61,
62, 63, 64, 65, 66, 67)

Director
Naval Research Laboratory
Washington, DC 20390
Attn: Code 8440
(Copy Nos. 68 and 69)

Ocean Structures Branch
U. S. Naval Research Laboratory
Washington, DC 20390
Attn: Dr. R. O. Belsheim
(Copy No. 70)

Office of Naval Research
Department of the Navy
Arlington, VA 22217
Attn: Dr. G. Boyer
Code 222
(Copy Nos. 71, 72, 73)

Office of Naval Research
Department of the Navy
Arlington, VA 22217
Attn: Dr. A. O. Sykes
Code 222
(Copy Nos. 74, 75, 76)

Office of Naval Research
Department of the Navy
Arlington, VA 22217
Attn: Mr. Keith M. Ellingsworth
Code 473
(Copy No. 77)

Office of Naval Research
Department of the Navy
Arlington, VA 22217
Attn: Dr. N. Perrone
Code 474
(Copy No. 78)

Commander
Mare Island Naval Shipyard
Vallejo, CA 94592
(Design Division)
(Copy No. 79)

Commander
Portsmouth Naval Shipyard
Portsmouth, NH 03801
(Copy No. 80)

Supervisor of Shipbuilding,
Conversion and Repair
General Dynamics Corporation
Electric Boat Division
Groton, CT 06340
Attn: Dr. Robert M. Gorman
Dept. 440
(Copy Nos. 81 and 82)

Supervisor of Shipbuilding,
Conversion and Repair
Ingalls Shipbuilding Corporation
Pascagoula, MS 39567
(Copy No. 83)

Supervisor of Shipbuilding,
Conversion and Repair
Newport News Shipbuilding and Drydock Company
Newport News, VA 23607
(Copy No. 84)

Naval Ship Research and
Development Center
Underwater Explosion Research
Division
Code 780
Portsmouth, VA 23709
(Copy No. 85)

Naval Underwater Systems Center
New London Laboratory
New London, CT 06320
Attn: Mr. G. F. Carey
(Copy No. 86)

Naval Underwater Systems Center
New London Laboratory
New London, CT 06320
Attn: Dr. R. S. Woollett
(Copy No. 87)

Naval Undersea Warfare Center
San Diego, CA 92152
Attn: Mr. G. Coleman
(Copy No. 88)

Dr. J. Barger
Bolt Beranek and Newman, Inc.
50 Moulton Street
Cambridge, MA 02138
(Copy No. 89)

Dr. D. I. G. Jones
Air Force Materials Laboratory
Wright-Patterson Air Force Base
Ohio 45433
(Copy No. 90)

Dr. M. C. Junger, President
Cambridge Acoustical Associates, Inc.
1033 Massachusetts Avenue
Cambridge, MA 02138
(Copy No. 91)

Acquisitions Supervisor
Technical Information Service
American Institute of Aeronautics
and Astronautics, Inc.
750 Third Avenue
New York, NY 10017
(Copy No. 92)

Dr. R. S. Ayre
Department of Civil Engineering
University of Colorado
Boulder, CO 80302
(Copy No. 93)

Dr. D. Frederick
Chairman, Engineering Science and Mechanics Department
Virginia Polytechnic Institute and State University
Blacksburg, VA 24061
(Copy No. 94)

Dr. D. E. Hudson
Department of Mechanics
California Institute of Technology
Pasadena, CA 91109
(Copy No. 95)

Dr. G. Herrmann, Chairman
Department of Applied Mechanics
Stanford University
Stanford, CA 94305
(Copy No. 96)

Dr. A. Kalnins
Department of Mechanical Engineering and Mechanics
Leheigh University
Bethlehem, PA 18015
(Copy No. 97)

Dr. D. D. Kana
Southwest Research Institute
8500 Culebra Road
San Antonio, TX 78206
(Copy No. 98)

Dr. Y. -H. Pao, Chairman
Department of Theoretical and Applied Mechanics
Cornell University
Ithaca
New York, NY 14850
(Copy No. 99)

Dr. J. R. Rice
School of Engineering
Brown University
Providence, RI 02912
(Copy No. 100)

Dr. P. S. Symonds
School of Engineering
Brown University
Providence, RI 02912
(Copy No. 101)

Dr. W. J. Worley
Department of Theoretical and Applied Mechanics
University of Illinois
Urbana, IL 61801
(Copy No. 102)

Dr. Dana Young
Southwest Research Institute
8500 Culebra Road
San Antonio, TX 78206
(Copy No. 103)

Commander
Naval Sea Systems Command
Department of the Navy
Washington, DC 20362
Attn: SEA-09G32-Library
(Copy Nos. 104 and 105)